ORGANOMETALLICS

pubs.acs.org/Organometallics Article

Redox Chemistry of Nickelocene-Based Monomers and Polymers

Rebecca A. Musgrave,* Andrew D. Russell, Paul R. Gamm, Rebekah L. N. Hailes, Kevin Lam, Hazel A. Sparkes, Jennifer C. Green, William E. Geiger,* and Ian Manners*

Cite This: *Organometallics* 2021, 40, 1945−1955 Read Online

ACCESS | Metrics & More | Article Recommendations | Supporting Information

ABSTRACT: The oxidation of [*n*]nickelocenophanes [Ni(η^5-C_5H_4)$_2$(CH_2)$_3$] (**3**), [Ni(η^5-C_5H_4)$_2$($SiMe_2$)$_2$] (**10**), [Ni(η^5-C_5H_4)$_2$($SiMe_2$)$_2$O] (**11**), [Ni(η^5-C_5H_4)$_2$(CH_2)$_4$] (**12**), and poly(nickelocenylpropylene) [Ni(η^5-C_5H_4)$_2$(CH_2)$_3$]$_n$ (**4**) to both the monocationic and dicationic species was investigated in dichloromethane by cyclic voltammetry (CV) and square-wave voltammetry. The presence of acetonitrile on the oxidation potentials of **3** in dichloromethane was also investigated by CV. The [*n*]nickelocenophanes **3** and **10**−**12** exhibited two single-electron Nernstian redox processes, and the monocations [**3**]$^+$, [**10**]$^+$, [**11**]$^+$, and [**12**]$^+$ were isolable as [B(C_6F_5)$_4$]$^-$ salts after chemical oxidation, and were structurally characterized. Ni−Cp_{cent} distances in all four monomers decreased upon oxidation, with a structural distortion manifested in the ring-tilt angle, α, among other angles. CV studies of the reversible first oxidation process to the polyelectrolyte {[Ni(η^5-C_5H_4)$_2$(CH_2)$_3$]$^+$}$_n$ ([**4**]$^{n+}$) were used to estimate the molecular weight of the polymeric material (M_w = 5300 g mol^{-1}) by comparing its diffusion coefficient with that of a monomeric analogue, and the second electrochemical oxidation of polymer **4** was found to be only partially chemically reversible.

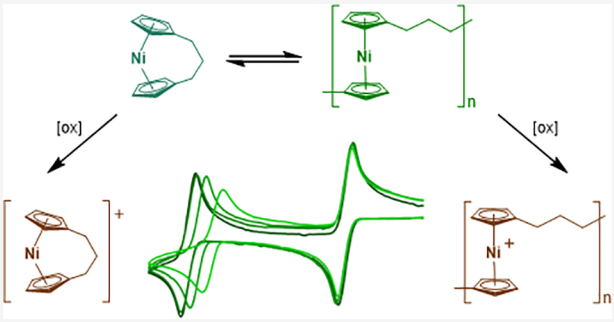

INTRODUCTION

The rich redox chemistry of metallocenes is exemplified by ferrocene (FcH), which possesses a reversible one-electron oxidation [FcH]$^+$/FcH at 0.64 V versus the standard hydrogen electrode (SHE) and is used as a reliable standard in electrochemistry.[1] Paramagnetic decamethylcobaltocene, [Co(η^5-C_5Me_5)$_2$], which exhibits a reduction potential of −1.94 V versus FcH, is commonly used as a strong reducing agent.[1] Both oxidation to the monocationic "metallocenium" and further oxidation to the dicationic species have only been observed for the metallocenes of iron, cobalt, and nickel. Very positive potentials (1.71 and 2.72 V versus FcH, respectively) are required to access the dication of ferrocene and cobaltocene via cyclic voltammetry (CV),[2,3] and the resulting 16 and 17 VE (valence electron) species are highly electrophilic and oxidizing.[4] 20 VE nickelocene (**1**) can be oxidized to both the monocationic 19 VE nickelocenium ion (**2**) and the respective 18 VE dicationic species, which is thermodynamically more accessible than related iron and cobalt species (requiring a potential of 1.06 V versus FcH).[5]

Polymers based on redox-active metallocenes have attracted considerable interest from a materials science perspective.[6−9] Recently, we reported numerous macromolecular systems based on nickelocene-containing repeat units.[10−12] These involve the ring-opening polymerization (ROP) of a cyclic [*n*]-nickelocenophane monomer such as **3** to yield poly(nickelocenylpropylene) **4** (Figure 1).[13] The lability of the Ni−Cp bonds (Cp = cyclopentadienyl) in both the moderately strained monomer (**3**) and the polymer (**4**) results in a system that is dynamic in nature, where at a low concentration or at an elevated temperature in a coordinating or polar solvent, depolymerization occurs.[12] Although this provides useful insight into the thermodynamic propensity for ROP in the strained

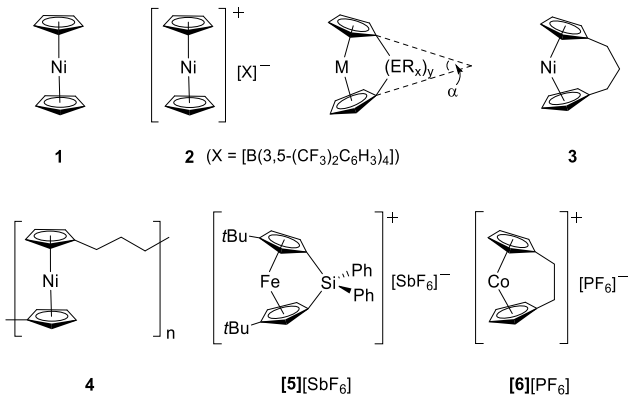

Figure 1. Metallocene-containing molecules.

Received: April 22, 2021
Published: June 18, 2021

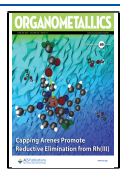

https://doi.org/10.1021/acs.organomet.1c00247
Organometallics 2021, 40, 1945−1955

monomer (**3**: $\Delta H^0_{ROP} = -10$ kJ mol^{-1}, $\Delta S^0_{ROP} = -21$ J K^{-1} mol^{-1}, $\Delta G^0_{ROP} = -4.0$ kJ mol^{-1} at 20 °C), it renders the polymeric material difficult to characterize and process as a result of its facile depolymerization in common solvents.

The oxidation of nickelocene (**1**) to the nickelocenium cation in **2** involves a decrease in metal−Cp bond length (**1**: Ni−Cp$_{cent}$ = 1.8167(13) Å, **2**: Ni−Cp$_{cent}$ = 1.700(4) Å) and a presumed increase in bond strength (cent = centroid).[14,15] The strengthening of Ni−Cp bonds in neutral polymers via the oxidation of nickelocene units to nickelocenium cations may render the resulting polyelectrolyte static and, therefore, stable to depolymerization. The ROP of novel strained [*n*]nickelocenophanium cations also provides an alternative route to these types of polyelectrolytes.

Several cationic [*n*]metallocenophanium ions (Figure 1) have been synthesized from various iron and cobalt [*n*]metallocenophanes,[16−20] and the structural and electronic effects upon oxidation are markedly different for each metal.[17] For example, the highly strained 17 VE silicon-bridged [1]ferrocenophanium ion ([**5**]$^+$) is synthesized via oxidation of the neutral 18 VE sila[1]ferrocenophane precursor **5**, and the tilt angle α (the dihedral angle between the two Cp rings; Figure 1) increases significantly (from 18.69(9)° to 28.9(13)°) as a result of the increase in the Fe−Cp$_{cent}$ distance.[20] This structural distortion can be related to the removal of a valence electron from the e′$_2$ bonding orbital in the ferrocene unit (Figure 2). In

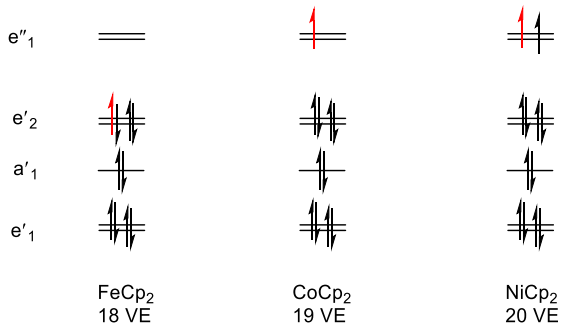

Figure 2. A simplified representation of the frontier molecular orbitals in metallocenes of Fe, Co, and Ni (neglecting the effects of zero-field splitting). Upon oxidation of the neutral metallocene to the monocationic species, the electron shown in red is removed.

contrast, upon oxidation of the 19 VE cobaltocene unit and removal of an electron from the e″$_1$ antibonding orbital (Figure 2), the opposite effect is observed.[16,18,19,21] [*n*]-Cobaltocenophanium ions (18 VE diamagnetic species) feature shorter Co−Cp$_{cent}$ distances and smaller tilt angles than their neutral precursors (e.g., dicarba[2]cobaltocenophanium [**6**]$^+$: α = 21.4(2)° as compared to the neutral dicarba[2]-cobaltocenophane **6**: α = 27.1(4)°).[18]

By contrast, the oxidation chemistry of [*n*]nickelocenophanes is far less explored. Nickelocene itself displays the reversible electrochemical sequence Ni^{II}/Ni^{III}/Ni^{IV} upon oxidation in a range of organic solvents, in addition to a reduction corresponding to a Ni^{II}/Ni^{I} redox couple, which is only partially chemically reversible.[2,22−24] The naphthalene-bridged [*n*]-nickelocenophane **7** (Figure 3) undergoes two oxidation processes as observed by CV, the first to the monocation, with electrochemical reversibility, and the second to the dication, which was only partially reversible.[25] A similar behavior was noted for the unsaturated tetracarba-bridged **8** (Figure 3).[26] The

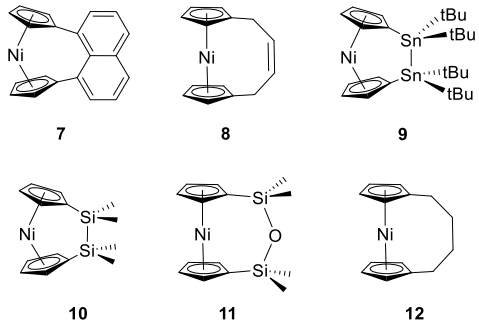

Figure 3. Examples of [*n*]nickelocenophanes **7**−**12**.

only isolated [*n*]nickelocenophanium ion is the distanna[2]-nickelocenophanium hexafluorophosphate salt ([**9**][PF$_6$]).[21] The 20 VE nickelocene unit in neutral **9** features two electrons occupying formally antibonding e″$_1$ orbitals (Figure 2). Oxidation affords the 19 VE nickelocenium species, where the Ni−Cp$_{cent}$ distance is decreased (**9**: α = 4.60 (8)°, Ni−Cp$_{cent}$ = 1.8141(8) Å, [**9**]$^+$: α = 3.67 (13)°, Ni−Cp$_{cent}$ = 1.7186(14) Å).[21] Further oxidation, to yield the 18 VE species [**9**]$^{2+}$, was demonstrated via CV[21] and is well-documented for related substituted nickelocenes.[5,22−24,27]

Currently, the ROP of [*n*]metallocenophanium cations has not been demonstrated. Although the sila[1]ferrocenophanium ion [**5**]$^+$ is highly strained, efforts to polymerize this monomer resulted in a thermally induced fluoride transfer reaction with its [SbF$_6$]$^-$ anion.[20] A thermal treatment of diaryl-substituted dicarba[2]cobaltocenophanium cations again does not lead to ROP but to a rupture across the dicarba bridge.[28] Recently, our group has reported the ROP of neutral [*n*]nickelocenophanes **3**, **10**, and **12** under particularly mild conditions,[10−12] suggesting that oxidized [*n*]nickelocenophanium cations may also be susceptible to ring-opening reactions. [*n*]Nickelocenophanium cations bearing significant ring strain have not yet been realized synthetically, but the Ni−Cp bond in these 19 VE species is expected to be weaker than the analogous Co−Cp bond in charged [*n*]cobaltocenophanium ions, making these species interesting candidates for ROP.

In this report we detail an electrochemical investigation of four [*n*]nickelocenophanes and the synthesis of their respective [*n*]nickelocenophanium salts. In addition, we perform an electrochemical oxidation of the nickelocene-based polymer **4**.

■ RESULTS AND DISCUSSION

1. Electrochemistry of [*n*]Nickelocenophane Monomers. The electrochemical behavior of the four mononuclear complexes **3**, **10**, **11**, and **12** (Figures 1 and 3) was investigated in a dichloromethane solution, employing [NBu$_4$][B(C$_6$F$_5$)$_4$] as the supporting electrolyte (0.05 M). The syntheses of these neutral [*n*]nickelocenophanes all utilize a salt metathesis route, involving the reaction of a dilithiated "fly trap" ligand and nickel(II) salt.[12,29] Only oxidative processes to form the Ni^{III} and Ni^{IV} species of **3** and **10**−**12** were investigated, in attempts to strengthen the Ni−Cp bond upon oxidation and investigate these monomers as potential charged precursors for ROP.

The voltammetric responses for all four species were reproducible and are displayed in Table 1 (all electrochemical potentials are reported relative to the ferrocene/ferrocenium couple, [FcH]$^{0/+}$). Each complex exhibited two quasi-Nernstian one-electron oxidation waves, which obeyed the diagnostic criteria for diffusion-controlled redox processes (there was no

https://doi.org/10.1021/acs.organomet.1c00247
Organometallics 2021, 40, 1945−1955

Table 1. $E_{1/2}$ Values (V Versus FcH) for [n]Nickelocenophanes, Related Nickelocenes, and Poly(nickelocenylpropylene) in 0.05 M $[NBu_4][B(C_6F_5)_4]/CH_2Cl_2$

compound	$E_{1/2}(1)$ (V versus FcH) Ni^{II}/Ni^{III}	$E_{1/2}(2)$ (V versus FcH) Ni^{III}/Ni^{IV}	$\Delta E_{1/2}$[a] (V)	ref
7[b,c]	−0.52	0.49[d]	1.01	25
8[b,e]	−0.59	0.31[d]	0.90	26
9[b]	−0.52	0.49	1.01	21
3	−0.70	0.86	1.56	
10	−0.46	0.86	1.32	
11	−0.41	0.97	1.38	
12	−0.61	0.94	1.55	
4	−0.69 (−0.47)[f]	0.88	1.57	
$[Ni(\eta^5\text{-}C_5H_5)_2]$	−0.46	1.06	1.52	5
$[Ni(\eta^5\text{-}C_5H_4Me)_2]$ (estimated)[g]	(−0.56)	(0.96)	(1.52)	31
$[Ni\{\eta^5\text{-}C_5H_4(SiMe_3)\}_2]$ (estimated)[h]	−0.44	1.04	1.48	31

[a] $\Delta E_{1/2} = E_{1/2}(2) - E_{1/2}(1)$. [b] $[Bu_4N][PF_6]$ electrolyte used. [c] CV performed in acetonitrile. [d] Second step only partially reversible. [e] CV performed in THF. [f] Smaller feature: see discussion. [g] Values for $[Ni(\eta^5\text{-}C_5H_4Me)_2]$ are estimated based on a negative shift of 0.05 V per methyl group. [h] Values for $[Ni\{\eta^5\text{-}C_5H_4(SiMe_3)\}_2]$ are estimated based on a positive shift of 0.01 V per $SiMe_3$ group.

evidence of adsorption onto the electrode surface by the analytes or their anodic products). The first wave corresponds to an oxidation of the [n]nickelocenophane (Ni^{II}, 20 VE) to the monocation (Ni^{III}, 19 VE), and the second corresponds to a further one-electron oxidation to the dication (Ni^{IV}, 18 VE) as shown in Scheme 1.

Scheme 1. Reversible One-Electron Oxidation Processes for Nickelocene-Based Molecules to the Respective Monocation and Dication[a]

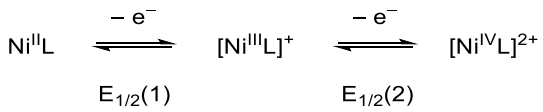

[a] "L" denotes the bridged Cp-based ligand backbone.

A representative CV scan for disila-bridged **10** (Figure 4a) demonstrates two redox processes at $E_{1/2} = -0.41$ and 0.97 V versus FcH. All of the redox processes for **3**, **10**, **11**, and **12** exhibit i_c/i_a (i_c = peak cathodic current, i_a = peak anodic current) values near unity for CV scan rates between 1.0 and 0.2 V s^{-1}, indicating full chemical reversibility of both oxidation processes on the voltammetric time scale. CV scans of compound **3** at low temperature (258 K) also exhibit full reversibility (Figure S1). Square-wave (SW) voltammograms were also recorded for each redox process. Although the peak widths at half-maximum are somewhat greater than expected (see Figure 4b for an example scan of **11**), the SW scans were also consistent with one-electron quasi-Nernstian redox processes. Previous investigations of the redox behavior of [n]nickelocenophanes **7** and **8** showed only a partial reversibility of the Ni^{III}/Ni^{IV} couple; a difference that is probably attributable to the nature of the electrolyte anion ($[PF_6]^-$, which is known to react with sufficiently electrophilic complexes) compared to the $[B(C_6F_5)_4]^-$ anion used in this study.[25,26,30]

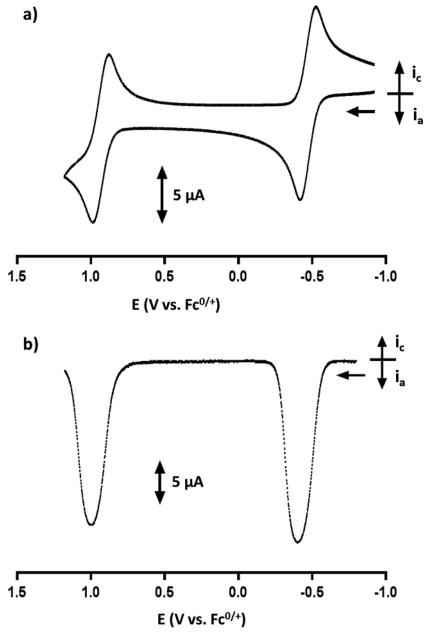

Figure 4. (a) Cyclic voltammogram for **10** (2 mM) in 0.05 M $[NBu_4][B(C_6F_5)_4]/CH_2Cl_2$ with a 2 mm glassy carbon electrode (gce), scan rate 0.2 V s^{-1}, T = 295 K. (b) SW voltammogram (60 Hz) for **11** (2.5 mM) in 0.05 M $[NBu_4][B(C_6F_5)_4]/CH_2Cl_2$ with a 2 mm gce, T = 295 K.

To aid the comparison with the parent nickelocene, the reported potentials of **1** in this medium (dichloromethane)[5] were adjusted to take into account the standard shift in $E_{1/2}$ introduced by the replacement of a ring proton with a methyl group (Table 1).[31] There is a significant thermodynamic stabilization (ca. 140 mV) of the tricarba-bridged Ni^{III} monocation $[\mathbf{3}]^+$ versus $[Ni(\eta^5\text{-}C_5H_4Me)_2]^+$, which is far less pronounced in the related tetracarba-bridged species $[\mathbf{12}]^+$ (ca. 50 mV). Otherwise, the potentials of the first (Ni^{II}/Ni^{III}) oxidations fall within a range that is consistent with normal ring substituent effects (substitution of the Cp ring with silicon results in a positive shift of only 0.01 V per $SiMe_3$ group introduced).[31] The potentials of the second couple (Ni^{III}/Ni^{IV}) of the hydrocarbon-bridged species display a similar trend to that of the first couple (Ni^{II}/Ni^{III}). The Ni^{IV} dication $[\mathbf{3}]^{2+}$ again exhibits a significant thermodynamic stabilization (ca. 100 mV) compared to $[Ni(\eta^5\text{-}C_5H_4Me)_2]^{2+}$, whereas for $[\mathbf{12}]^{2+}$ this stabilization is reduced to ca. 20 mV. A stabilization effect is also observed for the disila/siloxane-bridged species within this second redox couple. The dication of the disila-bridged compound $[\mathbf{10}]^{2+}$ exhibits a greater stabilization versus the $[Ni\{\eta^5\text{-}C_5H_4(SiMe_3)\}_2]^{2+}$ dication (180 mV) than that of siloxane-bridged $[\mathbf{11}]^{2+}$ (100 mV).

In general, it seems that a trend is observed between an increased thermodynamic stabilization of the cations and an increased tilt angle α. In a comparison of the hydrocarbon-bridged species, neutral **3** is significantly more tilted than **12** (α = 16.6° and 1.0°, respectively), and for the silicon-containing bridges, **10** is more tilted than **11** (α = 9.4° versus 3.5°). This increased tilt/stabilization relationship has also been observed in work by Braunschweig et al.,[21] and although the effect of tilting on the frontier orbitals in ferrocene is well-understood,[32] further theoretical investigation is required to justify this observation in *ansa*-nickelocenes.

https://doi.org/10.1021/acs.organomet.1c00247
Organometallics 2021, 40, 1945−1955

To provide further insight into the effect of Cp ring tilt on the ease of oxidation in these monomers, computational studies (see the Supporting Information for details) were performed to compare the first oxidation potential of hydrocarbon-bridged species, where the electronic influence of the bridge is expected to be similar across the three species probed. Both the tricarba- and tetracarba-bridged monomers **3** and **12** were investigated as well as the theoretical dicarba[2]nickelocenophane **13** (see Supporting Information, Table S2), the synthesis of which has not yet been realized. The calculations correctly predict that the one-electron oxidation of the neutral 20 VE [*n*]-nickelocenophane is more facile for tricarba-bridged **3** than tetracarba-bridged **12** (Table 2). The expected lowering of oxidation potential with increased tilt is, however, not observed for the theoretical molecule **13**, which features a calculated tilt angle of ca. 33°. The calculated value for the first oxidation to [**13**]$^+$ is −0.50 V versus FcH, suggesting that this highly strained species is more easily oxidized than its longer-bridged analogues (Table 2).

Table 2. Experimental and Calculated $E_{1/2}$ Values (*V* Versus FcH) for Hydrocarbon-Bridged [*n*]Nickelocenophanes

compound	tilt angle (deg)	experimental values		calculated values
		$E_{1/2}(1)$ (V versus FcH)	$E_{1/2}(2)$ (V versus FcH)	$E_{1/2}(1)$ (V versus FcH)
13	33[a]			−0.50
3	16.6	−0.70	0.86	−0.75
12	1.0	−0.61	0.94	−0.64

[a]Determined from an optimized structure.

It has been previously shown that the separation between the Ni^{II}/Ni^{III} and Ni^{III}/Ni^{IV} oxidation potentials, $\Delta E_{1/2}$ [$=E_{1/2}(2) - E_{1/2}(1)$], for nickelocene is very solvent-sensitive,[5] with large increases in oxidation potential (as much as 0.5 V) accompanying a decrease in solvent donor strength. This effect is demonstrated for the oxidation of **3** in dichloromethane (Figure 5). An increased acetonitrile content of the solution has little effect on the value of $E_{1/2}(1)$ but results in a significant decrease in the value of $E_{1/2}(2)$ corresponding to the oxidation to the dication (0.86 V without MeCN versus 0.59 V with 10%/vol MeCN). The value of $\Delta E_{1/2}$ therefore also decreases with increasing acetonitrile content, indicative of a thermodynamic stabilization of the electrophilic dication via the formation of solvent adducts. In addition, as the acetonitrile content increases, the oxidation and reduction peaks of Ni^{III}/Ni^{IV} are of lower intensity than the Ni^{II}/Ni^{III} couple, indicating either slower charge transfer or a further chemical reaction with the solvent, which is coupled to the second redox process.

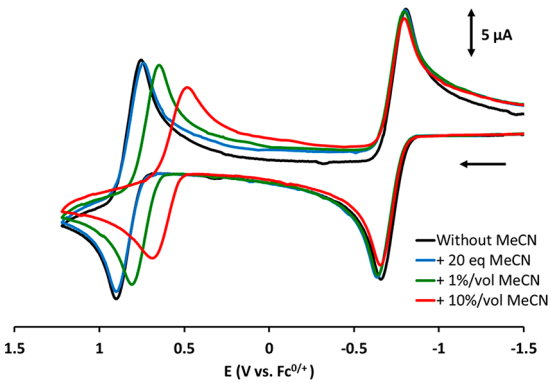

Figure 5. Cyclic voltammogram for **3** (1 mM) in 0.05 M $[NBu_4][B(C_6F_5)_4]/CH_2Cl_2$ with additional MeCN, scan rate 0.2 V s^{-1}, T = 295 K.

The large $\Delta E_{1/2}$ values observed when dichloromethane is employed as the solvent correlate with increased kinetic stabilities for the nickelocene dication. The $\Delta E_{1/2}$ values measured for the hydrocarbon-bridged [*n*]nickelocenophanes (**3** and **12**: 1.56 and 1.55 V, respectively) are similar to that of the parent nickelocene (1.52 V). The lower $\Delta E_{1/2}$ values for the disila/siloxane-bridged complexes **10** and **11** (1.32 and 1.38 V, respectively) may indicate a stronger solvation or ion-pairing interaction with the Ni^{IV} dications, but they still fall within a range in which the Ni^{IV} complex is kinetically stable. As can be seen in Table 1, the previously reported $\Delta E_{1/2}$ values for [*n*]nickelocenophanes with an unsaturated carbon or tin-based bridges (**7**, **8**, and **9**) are even smaller. The second oxidation potential of these complexes, in particular, is far more negative than the other [*n*]nickelocenophanes, and this is attributed to the electronic influence of the bridge, which renders the nickel center more electron-rich.[25,26]

The kinetic stabilities of the oxidized [*n*]nickelocenophanes (both monocationic and dicationic) were confirmed by bulk electrolysis experiments at 20 °C. For example, neutral **11** was oxidized at an applied voltage (E_{appl}) of 1.25 V (sufficient to oxidize the complex to the dication) with a two-electron process being confirmed by the net coulomb count (n_{app} = 1.8 e^-, 95% electrolysis). Linear scan voltammograms taken after the completion of the oxidation process confirmed the presence of the dication in solution, and the neutral complex was regenerated by cathodic back-electrolysis at E_{appl} = −1.0 V.

The CV scan in Figure 6 was recorded after this two-electron anodic electrolysis of **11**. In addition to showing the dominance of [**11**]$^{2+}$ in solution, it reveals the presence of a small wave (ca. −0.7 V), which presumably appears as a result of a side reaction of the [**11**]$^{2+}$ dication.[33] The Ni^{IV} dications of these [*n*]-nickelocenophanes are expected to be sensitive to attack by trace water or other adventitious nucleophiles, as similar observations have been made for the parent nickelocene dication.[34]

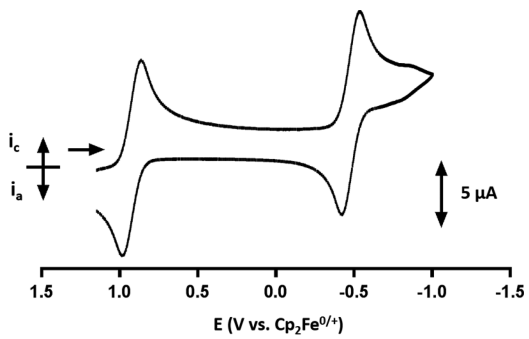

Figure 6. Cyclic voltammogram after bulk anodic oxidation of **11** (1.5 mM) at E_{appl} = 1.25 V in 0.05 M $[NBu_4][B(C_6F_5)_4]/CH_2Cl_2$ with a 2 mm gce, scan rate 0.2 V s^{-1}, T = 295 K.

2. Electrochemistry of Poly(nickelocenylpropylene). An investigation of the anodic behavior of poly(nickelocenylpropylene) **4**, which possesses one nickelocene-based moiety per repeat unit, showed main electrochemical features that are similar to those of the [*n*]nickelocenophane monomers. Thus, two apparent one-electron oxidations were

https://doi.org/10.1021/acs.organomet.1c00247
Organometallics 2021, 40, 1945−1955

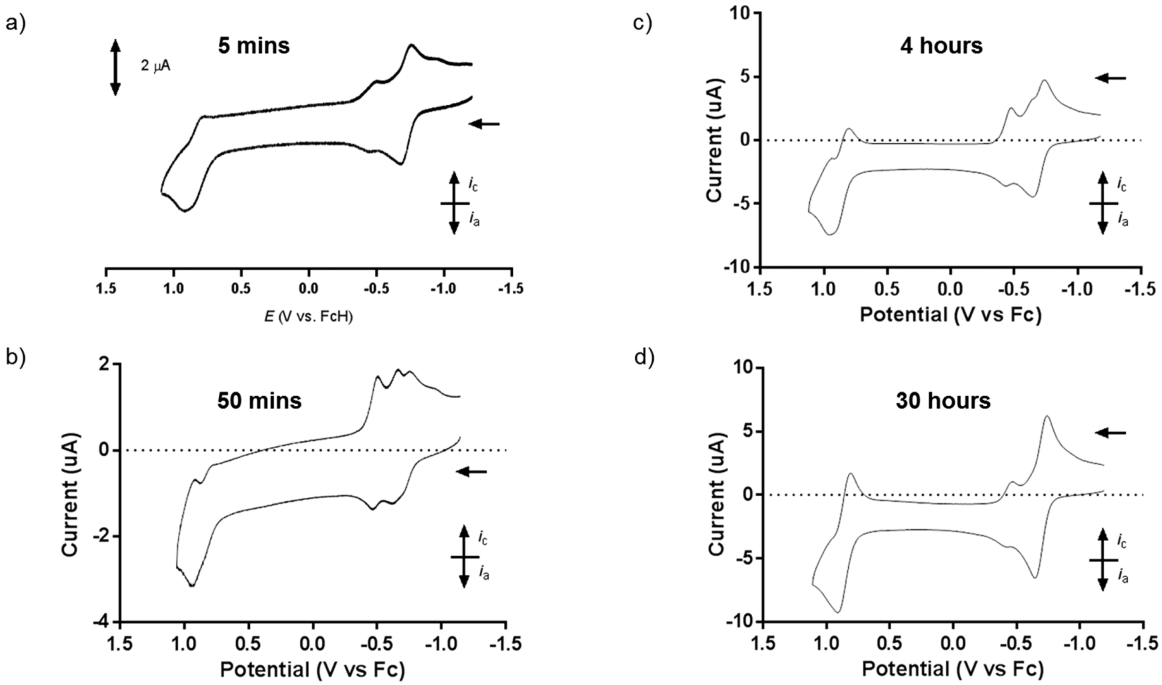

Figure 7. Cyclic voltammograms for **4** (0.5 mM) in 0.05 M $[NBu_4][B(C_6F_5)_4]/CH_2Cl_2$ with a 2 mm gce, scan rate 0.2 V s^{-1}, T = 295 K, at time, t = (a) 5 min, (b) 50 min, (c) 4 h, and (d) 30 h after dissolution of the polymer.

detected for the polymer in dichloromethane at $E_{1/2}$ values of −0.69 and 0.88 V in the cyclic voltammogram (Figure 7a), corresponding to formal Ni^{II}/Ni^{III} and Ni^{III}/Ni^{IV} redox couples of the nickelocenylpropylene repeat unit, respectively (Scheme 2).

Scheme 2. Oxidation of Polynickelocene 4 to Polyelectrolytes with Monocationic and Dicationic Repeat Units

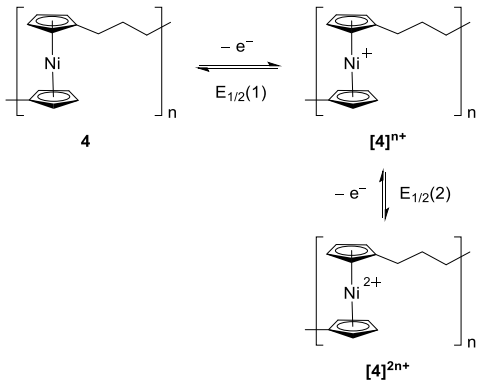

Although the Ni^{III}/Ni^{IV} wave (involving the oxidation of $[\mathbf{4}]^{n+}$ to $[\mathbf{4}]^{2n+}$) exhibits some chemical reversibility, the process is significantly less reversible than that of its precursor monomer **3**. The small cathodic feature on the reverse scan at $E_{pc} \approx -0.93$ V is thus ascribed to a follow-up reaction after the formation of the highly reactive dicationic Ni^{IV} species. The increased reactivity of the dicationic polymer $[\mathbf{4}]^{2n+}$ can be explained by the close proximity of Ni^{2+} centers along the chain relative to the independent solvated $[\mathbf{3}]^{2+}$ monomeric dications.

In addition to the two expected redox processes at −0.69 and 0.88 V (for the Ni^{II}/Ni^{III} and Ni^{III}/Ni^{IV} couples), an additional smaller feature was present at $E_{1/2}$ = −0.47 V, which may be assigned to either (1) the oxidation of nickel centers within the polymer chain, which are electronically distinct, or (2) the presence of an additional product in the polymer sample. The first possibility involving distinct nickel centers is feasible for a number of reasons, including the likely presence of both linear and cyclic material[12] and the difference in electronic environment of nickel centers in the center of the polymer chain versus at either end (for a linear material). However, a more convincing argument for the latter case involving an additional independent species can be made based on the effects of increased CV scan rates on this system. At higher scan rates, the cathodic portion of this small feature at −0.47 V shows a sharp spike, indicative of an adsorption-controlled process. However, the second major wave at 0.88 V remains diffusion-controlled, indicating the essential independence of these redox processes. Although the feature at −0.47 V cannot be assigned to either the monomer or polymer, its identity is unclear.

As determined previously, the dichloromethane solvent allows for significant depolymerization of **4** over time (Figure S14),[12] with some occurring in the first hour (at which time 10% of **4** has depolymerized). Monomer **3** and its respective polymer **4** exhibit similar redox potentials for both the Ni^{II}/Ni^{III} and Ni^{III}/Ni^{IV}couples (−0.70/−0.69 and 0.86/0.88 V, respectively), so the relative quantities of **3** and **4** in solution cannot be definitively determined based on $E_{1/2}$ values. However, kinetic studies were performed in which the electrochemical profile of a dilute dichloromethane solution of **4** was monitored over time (Figure 7a−d). Regarding the first oxidation at −0.69 V, the peak current increases over the time span of these experiments, the oxidation remains reversible, and the pre- and postpeaks diminish or disappear, respectively, over time. The small feature at −0.47 V does not appear to change much over time. Regarding the second oxidation at 0.88 V, the anodic peak current increases over time, and the reversibility also increases over time.

These observations are consistent with two processes occurring over time: (1) the polymer is slowly dissolving and

https://doi.org/10.1021/acs.organomet.1c00247
Organometallics 2021, 40, 1945−1955

(2) the polymer is depolymerizing. The anodic peak currents of the first and second oxidations increase over time as a result of the increased concentration of polymer upon its dissolution, and the reversibility of the second oxidation increases over time as the polymer depolymerizes to form monomer **3**. The pre- and postpeaks near the first oxidation diminish over time, as the second oxidation of the monomer is reversible, and therefore no follow-up reactions occur.

An estimate of the molecular weight of polymer **4** can be made, based on its apparent diffusion coefficient (D), compared with that measured for a monomeric analogue. This approach was originally described for poly(vinylferrocenes)[35] and more recently employed for ferrocene-based polyesters with the same electrolyte, $[NBu_4][B(C_6F_5)_4]$, as used in this case.[36] It relies on the interpretation of simple statistics for molecules that contain n identical, noninteracting centers (where each center has the same potential and adheres to the Nernst equation). The shape of the current−potential curve for the polymer has the same shape as that of a species where $n = 1$, but the diffusion-limiting current is larger by a factor of the degree of polymerization, n. Eq 1 can be used to determine n by relating the diffusion coefficients for the monomer and polymer (D_m and D_p, respectively).

$$n = \left(\frac{D_m}{D_p}\right)^{1.8} \tag{1}$$

Diffusion coefficients for the nickel complexes were evaluated by employing the Cottrell equation (eq 2) to evaluate chronoamperometry data obtained with a step time of five seconds for a species j (see the Supporting Information for details).[37]

$$i = \frac{nFAc_j^0\sqrt{D_j}}{\sqrt{\pi t}} \tag{2}$$

Values of 9.2×10^{-6} and 1.6×10^{-6} cm^2 s^{-1} were obtained for **11** and **4**, respectively, in 0.05 M $[NBu_4][B(C_6F_5)_4]/CH_2Cl_2$. These values were employed in eq 1 to estimate the molecular weight (assuming that the monomers **11** and **3** exhibit very similar diffusion coefficients). Polymer **4** is predicted to have a molecular weight of 5300 g mol^{-1} by this method and a corresponding degree of polymerization of 23. This molecular weight is significantly lower than the absolute molecular weight calculated by small-angle X-ray scattering (SAXS) (M_w = 20 000 g mol^{-1}),[12] and therefore it is likely that the polymer has undergone significant depolymerization over the time span of the CV experiment.

3. Synthesis of [*n*]Nickelocenophanium Salts. Three [n]nickelocenophanium cations were prepared via the respective oxidations of monomers **3**, **10**, and **11** with $[AcFc][B(C_6F_5)_4)]$ in dichloromethane (AcFc = acetylferrocene) (Scheme 3). $[AcFc][B(C_6F_5)_4)]$ exhibits a formal redox potential of 0.27 V versus FcH in this solvent[1] and is, therefore, a suitable oxidant to target these one-electron oxidation products (oxidation potentials of **3**, **10**, and **11** are −0.70, −0.46, and −0.41 V versus FcH, respectively).

An immediate color change from green to orange/brown was observed in all cases upon addition of the oxidant, as the neutral 20 VE [n]nickelocenophanes were oxidized to the respective cationic 19 VE [n]nickelocenophanium tetrakis(pentafluorophenyl)borate salts. UV−Visible spectroscopy (Supporting Information) showed that the lowest energy absorption for the cationic species is hypsochromically shifted

Scheme 3. Oxidation of [*n*]Nickelocenophanes 3, 10, and 11 to Form Respective [*n*]Nickelocenophanium Tetrakis(pentafluorophenyl)borate Salts

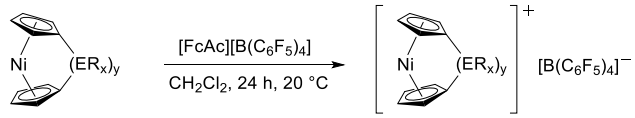

FcAc = Fe(η^5-C_5H_4)(η^5-$C_5H_4C(O)CH_3$)

3: $(ER_x)_y = (CH_2)_3$ **[3]**[$B(C_6F_5)_4$]: $(ER_x)_y = (CH_2)_3$
10: $(ER_x)_y = (SiMe_2)_2$ **[10]**[$B(C_6F_5)_4$]: $(ER_x)_y = (SiMe_2)_2$
11: $(ER_x)_y = (SiMe_2)_2O$ **[11]**[$B(C_6F_5)_4$]: $(ER_x)_y = (SiMe_2)_2O$

relative to the neutral species (e.g., $[3]^+$: λ_{max} = 434 nm (ε = 1584 M^{-1} cm^{-1}), **3**: λ_{max} = 673 nm (ε = 220 M^{-1} cm^{-1})[13]). The products were washed with hexanes to remove the neutral orange acetylferrocene side product. The cation of tetracarba[4]nickelocenophane **12** was instead prepared via an oxidation with the arylaminium salt $[N(C_6H_4Br\text{-}4)_3][B(C_6F_5)_4]$ to afford the corresponding tetrakis(pentafluorophenyl)borate salt (Scheme 4).

Scheme 4. Oxidation of Tetracarba[4]nickelocenophane 12 to Form the Tetrakis(pentafluorophenyl)borate Salt

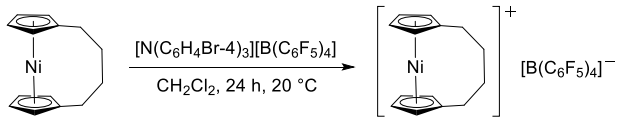

12 **[12]**[$B(C_6F_5)_4$]

^{1}H NMR spectroscopy of the [n]nickelocenophanium salts revealed broad signals assignable to α- and β-Cp proton environments in the paramagnetic region of the spectrum ([**3**][$B(C_6F_5)_4$]: −36.6 and −62.9 ppm, [**10**][$B(C_6F_5)_4$]: −30.8 and −113.6 ppm, [**11**][$B(C_6F_5)_4$]: −55.8 and −112.1 ppm, [**12**][$B(C_6F_5)_4$]: −74.5 and −178.0 ppm, respectively) shown in Figures S2−S5. These Cp resonances are observed much further downfield than those of their neutral [n]nickelocenophane precursors (ranging from −225 to −275 ppm) and are in a similar region to those observed for [**9**][PF_6] (−49 and −115 ppm). Protons of the $Si(CH_3)_2$ groups within the *ansa* bridges of $[\mathbf{10}]^+$ and $[\mathbf{11}]^+$ were also observed in the diamagnetic region of the spectrum at 8.9 and 4.8 ppm, respectively. Structural parameters for the four [n]nickelocenophanium $[B(C_6F_5)_4]^-$ salts are summarized in Table 3.

Brown/orange single crystals of [**3**][$B(C_6F_5)_4$] suitable for single-crystal X-ray diffraction were grown from a dichloromethane solution of the product at −40 °C. [**3**][$B(C_6F_5)_4$] crystallizes in the orthorhombic space group *Pbca* and exhibits disorder within the *ansa* bridge at C(7A)/C(7B). The molecular structure of $[\mathbf{3}]^+$ (Figure 8) reveals that the Ni−Cp_{cent} distances decrease on oxidation as expected (due to the removal of one electron from an e''_1 orbital) from 1.8045(av) Å (av = average) in **3** to 1.7075(av) Å in $[\mathbf{3}]^+$. As expected, a concomitant reduction in the tilt angle is observed (**3**: α = 16.6°; $[\mathbf{3}]^+$: α = 12.5(1)°) as the Ni−Cp_{cent} distance decreases and the structural constraints within the ring are relaxed (Table 3). The Cp rings within the metallocene unit are eclipsed, indicating that no additional strain is present as a result of torsional distortion.

Single crystals of [**10**][$B(C_6F_5)_4$] were grown by a slow diffusion of hexanes into a dichloromethane solution of the

https://doi.org/10.1021/acs.organomet.1c00247
Organometallics 2021, 40, 1945−1955

Table 3. Comparison of Important Structural Parameters of Compounds 3, 10, 11, and 12 and Their Respective Monocations[a]

	3	[3]$^+$	10	[10]$^+$	11	[11]$^+$	12	[12]$^+$
α (deg)	16.64(13)	11.4(3)	10.10(6)	9.35(9)	3.76(10)	2.6(2)	1.0(3)	−2.7(2)
β (deg)	4.2(3)	2.4(8)	11.39(10)	11.73(17)	5.0(2)	4.8(4)	0.5(6)	−3.3(5)
		4.9(7)	11.57(10)	11.59(15)	4.3(2)	4.3(4)	1.6(5)	−3.2(5)
δ (deg)	166.33(5)	170.23(18)	170.93(3)	171.84(2)	177.20(2)	177.56(7)	178.63(11)	178.04(11)
τ (deg)	N/A	N/A	12.12(2)	19.47(2)	N/A	N/A	45.6(2)	41.62(17)
Ni−Cp_{cent} (Å)	1.8051(14)	1.710(4)	1.8116(6)	1.7257(4)	1.8172(3)	1.714(2)	1.813(3)	1.729(2)
	1.8039(14)	1.705(4)	1.8131(7)	1.7271(4)	1.8180(3)	1.718(3)	1.817(3)	1.724(2)

[a]Geometric parameters are described in Figure 10 (α = dihedral angle between the plane of each Cp ring, β = [180° − (Cp_{cent}−C_{ipso}−E)] angle, δ = Cp_{cent}−Ni−Cp'_{cent} angle, τ = torsion angle between E−E and Cp_{cent}−Ni−Cp'_{cent} plane).

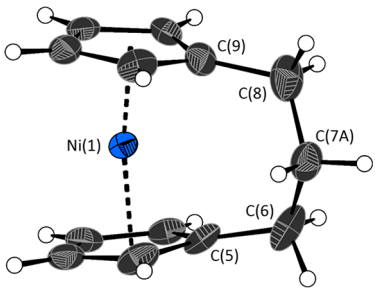

Figure 8. Molecular structure of the tricarba[3]nickelocenophanium cation [**3**]$^+$. Thermal ellipsoids displayed at the 50% probability level. Hydrogen atoms are pictured as spheres of arbitrary radii, and the $[B(C_6F_5)_4]^-$ counteranion was omitted. The *ansa* bridge is disordered at position C(7A). For clarity the position with the highest relative occupancy is displayed (62%). Selected distances (Å) and angles (deg): Ni(1)−Cp_{cent} 1.710(4)/1.705(4), C(9)−C(8)−C(7A) 117.1(3), C(6)−C(7A)−C(8) 119.6(4), C(5)−C(6)−C(7A) 116.8(3), α = 11.4(3), δ = 177.56(7).

product, which crystallizes in the monoclinic space group $P2_1/n$, and two views of the [**10**]$^+$ cation are shown in Figure 9. In a

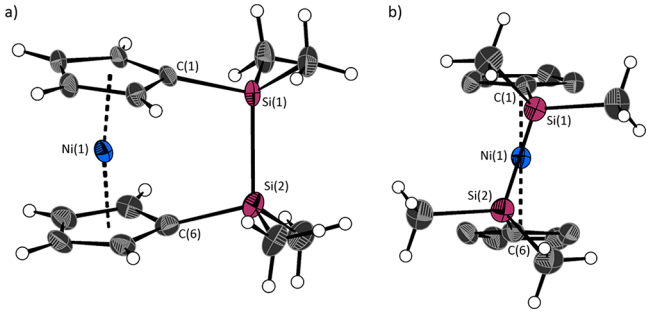

Figure 9. (a, b) Two views of the molecular structure of the tetramethyldisila[2]nickelocenophanium cation [**10**]$^+$. Thermal ellipsoids displayed at the 50% probability level. Hydrogen atoms are pictured as spheres of arbitrary radii (some are omitted for clarity), and the $[B(C_6F_5)_4]^-$ counteranion was omitted. Selected distances (Å) and angles (deg): Ni(1)−Cp_{cent} 1.7257(4)/1.7271(4), Si(1)−Si(2) 2.3635(10), C(1)−Si(1)−Si(2) 102.27(7), C(6)−Si(2)−Si(1) 103.12(7), α = 9.37(9), β = 168.27(17)/168.42(16), δ = 171.84(6).

similar manner to the tricarba-bridge species **3**, the Ni−Cp_{cent} distance decreases on oxidation, from 1.812(av) Å in **10** to 1.726(av) Å in [**10**]$^+$. However, the tilt angles in the two species are identical within error (**10**: α = 9.37(8)°; [**10**]$^+$: α = 9.37(9)°), which is unexpected, as a change in the M−Cp bond length usually has a significant effect on the tilt angle in [n]metallocenophanes. "Strain" is known to be expressed in more than one structural parameter, including δ (Cp_{cent}−M−Cp'_{cent}) and β (180° − [C_{cent}−C_{ipso}−E]). Upon closer examination, however, the δ angle is similar for both molecules (**10**: δ = 170.93(3)°; [**10**]$^+$: δ = 171.84(6)°), as are the sets of β angles (**10**: β = 168.43(10)/168.61(10)°; [**10**]$^+$: β = 168.27(17)/168.42(16)°). The Si−Si bond length within the bridge is also the same within error for both species (**10**: 2.3638(4) Å; [**10**]$^+$: 2.3636(10) Å).

The distortion that accounts for the structural differences between **10** and [**10**]$^+$ is manifested in a combination of τ (defined as the angle between the Si−Si bond of the bridge and the Cp_{cent}−Ni−Cp'_{cent} plane in the nickelocene unit) and ϕ (the extent to which the Cp ligands are staggered/eclipsed within the nickelocene unit) (Figure 10).

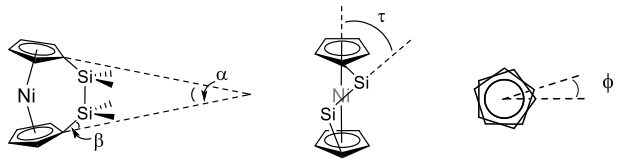

Figure 10. Angles depicting the structural parameters in [2]-nickelocenophanes (α = dihedral angle between the plane of each Cp ring, β = [180° − (Cp_{cent}−Cp_{ipso}−E)] angle, τ = torsion angle between E−E and Cp_{cent}−Ni−Cp'_{cent} plane, ϕ = torsion angle of Cp_{cent}−Cp_{ipso}−Cp'_{ipso}−Cp'_{cent}).

For the neutral species **10**, τ = 12.12(2)°, whereas for the cationic species [**10**]$^+$, it is much larger (τ = 19.47(2)°), indicating a greater twisting of the disila bridge to allow for some of the shortening of both Ni−Cp bonds. However, there is also a greater extent of "staggering" of the upper and lower Cp rings relative to one another (quantified by the torsion angle, ϕ; Cp_{ipso}−Cp_{cent}−Cp'_{cent}−Cp'_{ipso}), and this is far greater in cationic [**10**]$^+$ (ϕ = 12.86(15)°) than in neutral **10** (ϕ = 8.99(10)°), which contributes further to the overall twisting of the molecule upon oxidation. A very similar effect is observed in distanna[2]nickelocenophane **9** and its oxidation product [**9**]$^+$, where τ increases from 12.92(4)° to 24.56(4)° and staggering of the Cp rings (ϕ) also increases significantly from 11.00(12)° to 22.3(3)°.[21]

Compound [**11**][$B(C_6F_5)_4$] crystallizes in the monoclinic space group $P2_1/c$ and contains three formula units per asymmetric unit. One of these is disordered over the metallocene unit, the *ansa* bridge, and one of the C_6F_5 rings of the tetrakis(pentafluorophenyl)borate anion. The [**11**]$^+$ cation shown in Figure 11 (Ni(1)) exhibits no disorder, and the discussion will focus on this structure. The oxidation product again exhibits both a shortening of the Ni−Cp bonds (1.716(av) Å in [**11**]$^+$ versus 1.8176(av) Å in **11**) and a reduction in tilt angle (α = 2.6(2)° in [**11**]$^+$ versus 3.76(10)° in **11**). The

https://doi.org/10.1021/acs.organomet.1c00247
Organometallics 2021, 40, 1945−1955

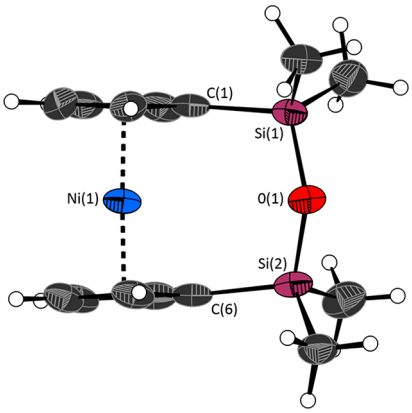

Figure 11. Molecular structure of the 1,3-tetramethyldisila-2-oxa[3]-nickelocenophanium cation [**11**]$^+$. Thermal ellipsoids displayed at the 50% probability level. Hydrogen atoms are pictured as spheres of arbitrary radii, and the $[B(C_6F_5)_4]^-$ counteranion was omitted. Selected distances (Å) and angles (deg): Ni(1)−Cp_{cent} 1.714(2)/1.718(3), Ni(1)···O(1) 3.530(4), Si(1)−O(1)−Si(2) 144.3(3), α = 2.6(2), δ = 177.56(7).

intramolecular Ni(1)···O(1) distance in [**11**]$^+$ (3.530(4) Å) is very similar to that of the neutral species **11** (3.5217(18) Å) and shows no interaction of the oxygen lone pairs with the nickel-based cation.

In a similar manner to that of [**10**][$B(C_6F_5)_4$], compound [**12**][$B(C_6F_5)_4$] was isolated via a slow diffusion of hexanes into a dichloromethane solution of the product. [**12**][$B(C_6F_5)_4$] crystallizes in the orthorhombic space group *Pbca* (Figure 12)

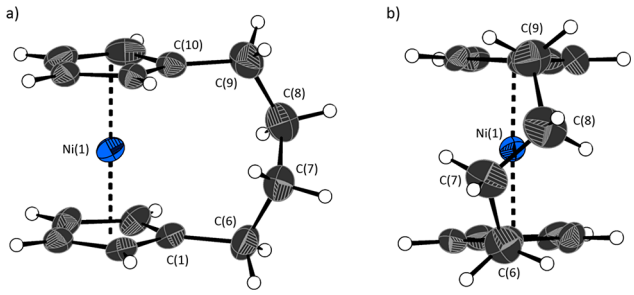

Figure 12. Molecular structure of the tetracarba[4]-nickelocenophanium cation [**12**]$^+$. Thermal ellipsoids displayed at the 50% probability level. Hydrogen atoms are pictured as spheres of arbitrary radii, and the $[B(C_6F_5)_4]^-$ counteranion was omitted. The *ansa* bridge is disordered at positions C(7) and C(8). For clarity the positions with the highest relative occupancy are displayed (85%). Selected distances (Å) and angles (deg): Ni(1)−Cp_{cent} 1.729(2)/1.724(2), α = −2.7(2), δ = 178.04(11).

and exhibits disorder within the *ansa* bridge at C(7)/C(7A) and C(8)/C(8A). The tilt angle α is nominally defined as the angle between the Cp rings, but for clarity in this text we will define alpha relative to the *ansa* bridge. Thus, unusually [**12**]$^+$ displays a negative tilt angle (α = −2.7(2)°); that is, the Cp rings tilt away from the *ansa* bridge. In comparison to the neutral analogue, the oxidation product exhibits shorter Ni−Cp bonds (1.727(av) Å in [**12**]$^+$ versus 1.815(av) Å in **12**), and the corresponding decrease in tilt angle from α = 1.0(3)° in **12** to a slightly negative value is therefore not unexpected. In addition, the decrease in Ni−Cp bond length gives rise to an inversion in tilt of the *ipso* carbons in the *ansa* bridge of [**12**]$^+$ compared to the neutral structure (β = −3.3°(av) for [**12**]$^+$ versus 1.1°(av) for **12**).

The preparation of [*n*]nickelocenophanium ions with a greater tilt is an attractive goal, and these species are expected to exhibit a greater stability than their neutral analogues, as can be appreciated in Figure 13. Calculations of the change in the

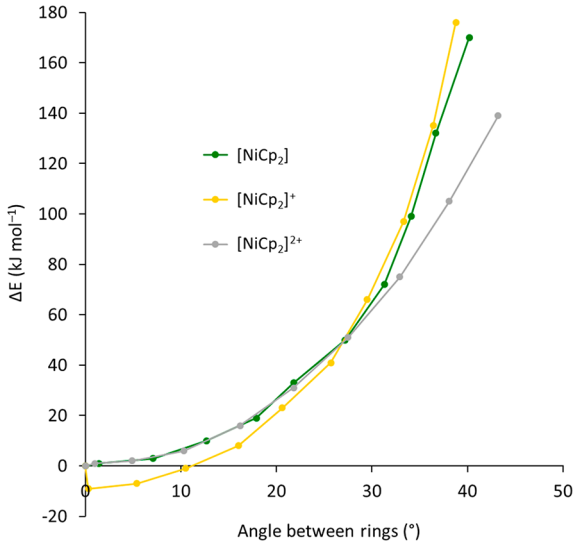

Figure 13. Variation of total energy of [$NiCp_2$], [$NiCp_2$]$^+$, and [$NiCp_2$]$^{2+}$ as a function of the tilt angle α.

total energy of the parent nickelocene [$NiCp_2$] and nickelocenium [$NiCp_2$]$^+$ versus tilt angle show that the total energy of the monocation lies below that for the neutral nickelocene until the tilt angle reaches ca. 28°. However, the only route to these cations at present involves the oxidation of neutral [*n*]-nickelocenophanes. The tricarba-bridged species **3** undergoes a spontaneous ROP, and as a result, the synthesis of the dicarba-bridged species **13** has been unsuccessful. As discussed, the naphthalene-bridged species **7** exhibits a greater tilt (α = 20.2°) than **3**, although the rigidity of the fused aromatic *ansa* bridge may account for the stability of this monomer toward ring-opening. We have, however, previously investigated the thermodynamic propensity of neutral [*n*]nickelocenophane monomers **3**, **10**, **11**, and **12** toward ring opening,[10] reporting that α is not always responsible for the ring strain in these monomers. Further modeling of [*n*]nickelocenophanium *ansa*-briged species may therefore be necessary, especially given the subtle differences in τ and ϕ for species **10** and [**10**]$^+$.

4. Attempted ROP of [*n*]Nickelocenophanium Cation [3]$^+$. The tilt angle of [**3**]$^+$ (α = 11.4(3)°), although smaller than it neutral precursor, may still be large enough to drive ring-opening chemistry via the release of strain. In an experiment similar to that of the ROP of **3**, [**3**][$B(C_6F_5)_4$] was dissolved in pyridine (0.11 M) and stirred for 24 h at room temperature, after which time no obvious color change was observed. A precipitation into hexanes was not a viable polymer isolation method in this case (as any remaining charged monomer would also precipitate from solution), so the solvent was removed in vacuo, and the product(s) were analyzed by ^{1}H NMR spectroscopy in dichloromethane-d_2. No signals corresponding to the starting material [**3**][$B(C_6F_5)_4$] could be observed, and the only shifts in the paramagnetic region of the spectrum appeared at 19.9, 10.9, and −8.3 ppm, which could not be assigned. A small amount of material was dissolved in tetrahydrofuran (THF) to perform dynamic light-scattering (DLS) experiments, which showed that material of size R_h = 1.8

https://doi.org/10.1021/acs.organomet.1c00247
Organometallics 2021, 40, 1945−1955

nm was present (Figure S12), although this could not conclusively be assigned to a polymeric material based on the $[\mathbf{3}]^+$ unit.

5. Oxidation of Polynickelocene 4. An alternative synthetic route to the $[\mathbf{4}]^{n+}$-based polyelectrolyte involves a chemical oxidation of the neutral polymer. Attempts were made to chemically oxidize polymer **4** to its monocationic repeat unit form in much the same way as for the monomeric complexes. The oxidation of **4** with 1 equiv of $[AcFc][B(C_6F_5)_4]$ in nitromethane-d_3 (Scheme 5, top) resulted in a color change from green to brown and the precipitation of a brown solid.

Scheme 5. Full and Partial Chemical Oxidation of Polymer 4 to Yield Polyelectrolytes $[\mathbf{4}][B(C_6F_5)_4]_n$ and $[\mathbf{4}][B(C_6F_5)_4]_{3n/4}$

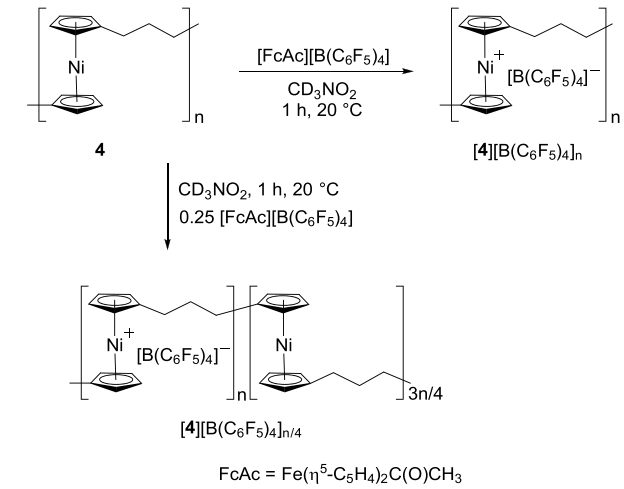

^{1}H NMR spectroscopy of the nitromethane-soluble product showed the presence of a small amount of cationic monomer, $[\mathbf{3}]^+$. The precipitate was dissolved in dichloromethane-d_2, and ^{1}H NMR spectroscopy of this solution exhibited a number of interesting features (Figure 14). First, there is no neutral polymer **4** present, and we can assume that it has been fully consumed during the oxidation. The broad singlets at −35.8 and −63.6 ppm indicate that a small amount of $[\mathbf{3}]^+$ is also present in solution (this could be a result of the depolymerization of the neutral polymer, followed by an oxidation, or vice versa). Most interestingly, the three larger resonances at −134.5, −88.3, and 37.0 ppm are shifted downfield relative to those of neutral nickelocenes and cannot be assigned to neutral monomer **3**, neutral polymer **4**, or cationic monomer $[\mathbf{3}]^+$. It is possible that these resonances correspond to Cp protons and β-CH_2 propyl protons in polyelectrolytic $[\mathbf{4}]^{n+}$ (in a similar manner to that of the neutral polymer, α-CH_2 propyl protons could not be assigned). To ascertain whether the material present was polymeric, DLS experiments were performed (Figure S13), and these indicated that material of size R_h = 3.8 nm was present in the solution, consistent with the formation of polyelectrolyte $[\mathbf{4}][B(C_6F_5)_4]_n$.

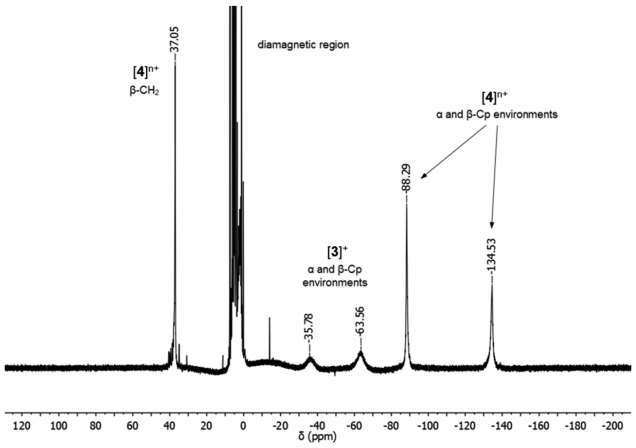

Figure 14. ^{1}H NMR spectrum (500 MHz, CD_2Cl_2) of $[\mathbf{4}][B(C_6F_5)_4]$ with the presence of $[\mathbf{3}][B(C_6F_5)_4]$.

SUMMARY

We have explored the electrochemistry of a number of [*n*]nickelocenophanes with carbon-, silicon-, and oxygen-containing *ansa* bridges, identifying oxidation events to monocationic and dicationic species by cyclic voltammetry. Monocationic species $[\mathbf{3}]^+$, $[\mathbf{10}]^+$, $[\mathbf{11}]^+$, and $[\mathbf{12}]^+$ were isolable as $[B(C_6F_5)_4]^-$ salts after a chemical oxidation, and they exhibited reduced $Ni-Cp_{cent}$ distances. The nickelocene-containing polymer **4** was also subjected to an electrochemical investigation, and the reversible first oxidation process to the polyelectrolyte $\{[Ni(\eta^5\text{-}C_5H_4)_2(CH_2)_3]^+\}_n$ ($[\mathbf{4}]^{n+}$) allowed for an estimation of the molecular weight of the polymeric material (M_w = 5300 g mol^{-1}) by a comparison of its diffusion coefficient with that of a monomeric analogue.

ASSOCIATED CONTENT

Supporting Information

The Supporting Information is available free of charge at https://pubs.acs.org/doi/10.1021/acs.organomet.1c00247.

Materials and equipment, experimental details, physical methods, NMR and UV−vis spectroscopic data, mass spectrometry and DLS data, computational methods, crystallographic tables (PDF)

Accession Codes

CCDC 2079224−2079227 contain the supplementary crystallographic data for this paper. These data can be obtained free of charge via www.ccdc.cam.ac.uk/data_request/cif, or by emailing data_request@ccdc.cam.ac.uk, or by contacting The Cambridge Crystallographic Data Centre, 12 Union Road, Cambridge CB2 1EZ, UK; fax: +44 1223 336033.

AUTHOR INFORMATION

Corresponding Authors

Rebecca A. Musgrave − *School of Chemistry, University of Bristol, Bristol BS8 1TS, U.K.;* Present Address: Department of Chemistry, King's College London, Britannia House, 7 Trinity Street, London, SE1 1DB, UK.; orcid.org/0000-0001-9404-0422; Email: rebecca.musgrave@kcl.ac.uk

William E. Geiger − *Department of Chemistry, University of Vermont, Burlington 05405-0125, Vermont, United States;* orcid.org/0000-0002-9152-8550; Email: william.geiger@uvm.edu

Ian Manners − *School of Chemistry, University of Bristol, Bristol BS8 1TS, U.K.; Department of Chemistry, University of Victoria, Victoria V8P 5C2, British Columbia, Canada;* orcid.org/0000-0002-3794-967X; Email: imanners@uvic.ca

https://doi.org/10.1021/acs.organomet.1c00247
Organometallics 2021, 40, 1945−1955

Authors

Andrew D. Russell − *School of Chemistry, University of Bristol, Bristol BS8 1TS, U.K.*

Paul R. Gamm − *Department of Chemistry, University of Vermont, Burlington 05405-0125, Vermont, United States*

Rebekah L. N. Hailes − *School of Chemistry, University of Bristol, Bristol BS8 1TS, U.K.;* orcid.org/0000-0001-8895-6426

Kevin Lam − *Department of Chemistry, University of Vermont, Burlington 05405-0125, Vermont, United States;* Present Address: School of Science, Department of Pharmaceutical Chemical and Environmental Sciences, University of Greenwich Central Avenue, Chatham Maritime, ME4 4TB, UK.; orcid.org/0000-0003-1481-9212

Hazel A. Sparkes − *School of Chemistry, University of Bristol, Bristol BS8 1TS, U.K.*

Jennifer C. Green − *Department of Chemistry, University of Oxford, Chemical Research Laboratory, Oxford OX1 3TA, U.K.*

Complete contact information is available at: https://pubs.acs.org/10.1021/acs.organomet.1c00247

Notes

The authors declare no competing financial interest.

■ ACKNOWLEDGMENTS

We thank the Engineering and Physical Sciences Research Council (EPSRC, EP/N030702/1) for funding. I.M. thanks the Government of Canada for a C150 Research Chair and the University of Bristol for support. W.E.G. thanks the National Science Foundation for support (NSF CHE-1565541).

■ REFERENCES

(1) Connelly, N. G.; Geiger, W. E. Chemical Redox Agents for Organometallic Chemistry. *Chem. Rev.* **1996**, *96*, 877−910.

(2) Bard, A. J.; Garcia, E.; Kukharenko, S.; Strelets, V. V. Electrochemistry of metallocenes at very negative and very positive potentials - Electrogeneration of 17-Electron Cp_2Co^{2+}, 21-electron Cp_2Co^{2-}, and 22-electron Cp_2Ni^{2-} species. *Inorg. Chem.* **1993**, *32*, 3528−3531.

(3) Sharp, P. R.; Bard, A. J. Electrochemistry in liquid sulfur dioxide. 4. Electrochemical production of highly oxidized forms of ferrocene, decamethylferrocene, and iron bis(tris(1-pyrazolyl)borate). *Inorg. Chem.* **1983**, *22*, 2689−2693.

(4) Malischewski, M.; Adelhardt, M.; Sutter, J.; Meyer, K.; Seppelt, K. Isolation and structural and electronic characterization of salts of the decamethylferrocene dication. *Science* **2016**, *353*, 678−682.

(5) Chong, D. S.; Slote, J.; Geiger, W. E. The role of solvent in the stepwise electrochemical oxidation of nickelocene to the nickelocenium dication. *J. Electroanal. Chem.* **2009**, *630*, 28−34.

(6) Hailes, R. L. N.; Oliver, A. M.; Gwyther, J.; Whittell, G. R.; Manners, I. Polyferrocenylsilanes: synthesis, properties, and applications. *Chem. Soc. Rev.* **2016**, *45*, 5358−5407.

(7) Liu, X.; Zhao, L.; Liu, F.; Astruc, D.; Gu, H. Supramolecular redox-responsive ferrocene hydrogels and microgels. *Coord. Chem. Rev.* **2020**, *419*, 213406.

(8) Cirelli, M.; Hao, J.; Bor, T. C.; Duvigneau, J.; Benson, N.; Akkerman, R.; Hempenius, M. A.; Vancso, G. J. Printing "Smart" Inks of Redox-Responsive Organometallic Polymers on Microelectrode Arrays for Molecular Sensing. *ACS Appl. Mater. Interfaces* **2019**, *11*, 37060−37068.

(9) Yang, P.; Pageni, P.; Kabir, M. P.; Zhu, T.; Tang, C. Metallocene-Containing Homopolymers and Heterobimetallic Block Copolymers via Photoinduced RAFT Polymerization. *ACS Macro Lett.* **2016**, *5*, 1293−1300.

(10) Musgrave, R. A.; Hailes, R. L. N.; Annibale, V. T.; Manners, I. Role of torsional strain in the ring-opening polymerisation of low strain [*n*]nickelocenophanes. *Chem. Sci.* **2019**, *10*, 9841−9852.

(11) Hailes, R. L. N.; Musgrave, R. A.; Kilpatrick, A. F. R.; Russell, A. D.; Whittell, G. R.; O'Hare, D.; Manners, I. Ring-Opening Polymerisation of Low-Strain Nickelocenophanes: Synthesis and Magnetic Properties of Polynickelocenes with Carbon and Silicon Main Chain Spacers. *Chem. - Eur. J.* **2019**, *25*, 1044−1054.

(12) Musgrave, R. A.; Russell, A. D.; Hayward, D. W.; Whittell, G. R.; Lawrence, P. G.; Gates, P. J.; Green, J. C.; Manners, I. Main Chain Metallopolymers at the Static-Dynamic Boundary Based on Nickelocene. *Nat. Chem.* **2017**, *9*, 743−750.

(13) Baljak, S.; Russell, A. D.; Binding, S. C.; Haddow, M. F.; O'Hare, D.; Manners, I. Ring-opening polymerization of a strained [3]-nickelocenophane: A route to polynickelocenes, a class of $S = 1$ metallopolymers. *J. Am. Chem. Soc.* **2014**, *136*, 5864−5867.

(14) Seiler, P.; Dunitz, J. D. The structure of nickelocene at room temperature and at 101 K. *Acta Crystallogr., Sect. B: Struct. Crystallogr. Cryst. Chem.* **1980**, *36*, 2255−2260.

(15) Priego, J. L.; Doerrer, L. H.; Rees, L. H.; Green, M. L. H. Weakly-coordinating anions stabilise the unprecedented monovalent and divalent eta-benzene nickel cations $[(\eta\text{-}C_5H_5)Ni(\eta\text{-}C_6H_6)Ni(\eta\text{-}C_5H_5)]^{2+}$ and $[Ni(\eta\text{-}C_6H_6)_2]^{2+}$. *Chem. Commun.* **2000**, 779−780.

(16) Drewitt, M. J.; Barlow, S.; O'Hare, D.; Nelson, J. M.; Nguyen, P.; Manners, I. The first [2]cobaltocenophane and [2]-metallocenophanium salts. *Chem. Commun.* **1996**, 2153−2154.

(17) Watanabe, M.; Sato, K.; Motoyama, I.; Sano, H. Mössbauer Studies of Bridged Ferrocenophane Derivative's Polyiodides. *Chem. Lett.* **1983**, *12*, 1775−1778.

(18) Mayer, U. F. J.; Charmant, J. P. H.; Rae, J.; Manners, I. Synthesis and Structures of Strained, Neutral and Cationic Hydrocarbon Bridged [*n*]Colboltocenophanes. *Organometallics* **2008**, *27*, 1524−1533.

(19) Braunschweig, H.; Breher, F.; Kaupp, M.; Gross, M.; Kupfer, T.; Nied, D.; Radacki, K.; Schinzel, S. Synthesis, Crystal Structure, EPR and DFT Studies, and Redox Properties of [2]-Tetramethyldisilacobaltocenophane. *Organometallics* **2008**, *27*, 6427−6433.

(20) Masson, G.; Herbert, D. E.; Whittell, G. R.; Holland, J. P.; Lough, A. J.; Green, J. C.; Manners, I. Synthesis and Reactivity of a Strained Silicon-Bridged [1]Ferrocenophanium Ion. *Angew. Chem., Int. Ed.* **2009**, *48*, 4961−4964.

(21) Arnold, T.; Braunschweig, H.; Damme, A.; Horl, C.; Kramer, T.; Krummenacher, I.; Mager, J. Tin-Bridged *ansa*-Metallocenes of the Late Transition Metals Cobalt and Nickel: Preparation, Molecular and Electronic Structures, and Redox Chemistry. *Organometallics* **2014**, *33*, 1659−1664.

(22) Wilson, R. J.; Warren, L. F.; Hawthorne, M. F. Existence of Nickel(IV) Dication Derived from Nickelocene and a Cationic Boron Hydride Analog. *J. Am. Chem. Soc.* **1969**, *91*, 758−759.

(23) Holloway, J. D. L.; Geiger, W. E. Electron-transfer reactions of metallocenes. Influence of metal oxidation state on structure and reactivity. *J. Am. Chem. Soc.* **1979**, *101*, 2038−2044.

(24) Koelle, U.; Khouzami, F. Permethylated Electron-Excess Metallocenes. *Angew. Chem., Int. Ed. Engl.* **1980**, *19*, 640−641.

(25) Trtica, S.; Meyer, E.; Prosenc, M. H.; Heck, J.; Böhnert, T.; Görlitz, D. Naphthalene-bridged ansa-nickelocene: Synthesis, structure, electrochemical, and magnetic measurements. *Eur. J. Inorg. Chem.* **2012**, *2012*, 4486−4493.

(26) Buchowicz, W.; Jerzykiewicz, L. B.; Krasińska, A.; Losi, S.; Pietrzykowski, A.; Zanello, P. *ansa*-Nickelocenes by the ring-closing metathesis route: Syntheses, X-ray crystal structures, and physical properties. *Organometallics* **2006**, *25*, 5076−5082.

(27) Wilkinson, G.; Pauson, P. L.; Cotton, F. A. Bis-Cyclopentadienyl Compounds of Nickel and Cobalt. *J. Am. Chem. Soc.* **1954**, *76*, 1970−1974.

(28) Mayer, U. F. J.; Manners, I., *Unpublished Results*.

(29) Braunschweig, H.; Gross, M.; Radacki, K. Synthesis, Molecular Structure, and Reactivity of the First Strained [2]Silanickelocenophane. *Organometallics* **2007**, *26*, 6688−6690.

(30) Brookhart, M.; Grant, B.; Volpe, A. F. $[(3,5\text{-}(CF_3)_2C_6H_3)_4B]$-$[H(OEt_2)_2]^+$ - a Convenient Reagent for Generation and Stabilization of Cationic, Highly Electrophilic Organometallic Complexes. *Organometallics* **1992**, *11*, 3920−3922.
(31) Lu, S. X.; Strelets, V. V.; Ryan, M. F.; Pietro, W. J.; Lever, A. B. P. Electrochemical parametrization in sandwich complexes of the first row transition metals. *Inorg. Chem.* **1996**, *35*, 1013−1023.
(32) C Green, J. Bent metallocenes revisited. *Chem. Soc. Rev.* **1998**, *27*, 263−271.
(33) This small feature was also observable in CV scans, which swept through the Ni(III)/Ni(IV) wave when the dichloromethane used for the experiment had not been rigorously dried (see the Supporting Information), and in these cases the Ni(III)/Ni(IV) wave exhibited a partial loss in reversibility.
(34) Vanduyne, R. P.; Reilley, C. N. Low-Temperature Electrochemistry 0.3. Application to Study of Radical Ion Decay Mechanisms. *Anal. Chem.* **1972**, *44*, 158−169.
(35) Flanagan, J. B.; Margel, S.; Bard, A. J.; Anson, F. C. Electron-Transfer to and from Molecules Containing Multiple, Noninteracting Redox Centers - Electrochemical Oxidation of Poly(Vinylferrocene). *J. Am. Chem. Soc.* **1978**, *100*, 4248−4253.
(36) Nafady, A.; McAdam, C. J.; Bond, A. M.; Moratti, S. C.; Simpson, J. Electrochemical studies with dissolved and surface-confined forms of *neo*-pentyl-ferrocene-based polyesters utilising $[NBu_4][B(C_6F_5)_4]$ and other electrolytes. *J. Solid State Electrochem.* **2009**, *13*, 1511−1519.
(37) Bard, A. J.; Faulkner, L. R. *Electrochemical Methods,* 2nd ed.; John Wiley & Sons: New York, 2001.

https://doi.org/10.1021/acs.organomet.1c00247
Organometallics 2021, 40, 1945−1955